EDINBURGH INSTRUMENTS

50 YEARS 1971-2021

PRECISION RAMAN

Best-in-class Raman microscopes
for research and analytical requirements backed with world-class customer support and service.

edinst.com

Research Article

Journal of RAMAN SPECTROSCOPY

Received: 3 July 2008 Accepted: 21 October 2008 Published online in Wiley Interscience: 19 December 2008

(www.interscience.wiley.com) DOI 10.1002/jrs.2166

FT-Raman and FT-IR spectral and quantum chemical studies on some flavonoid derivatives: Baicalein and Naringenin

Ozan Unsalan,[a]* Yusuf Erdogdu[b] and M. Tahir Gulluoglu[b]

In this study, the experimental and theoretical results on the molecular structures of some flavonoid derivatives (Baicalein and Naringenin) are presented. The FT-IR and FT-Raman spectra of the compounds have been recorded together for the first time between 4000–400 cm^{-1} and 3500–5 cm^{-1} regions, respectively. The molecular geometry and vibrational wavenumbers of the compounds have been also calculated in their ground states by using *ab initio* HF and DFT/B3LYP functional with 6-31G(d,p) basis set used in calculations. The calculations were utilized to the C_1 symmetries of the molecules. All calculations were performed with Gaussian 98 software. The obtained vibrational wavenumbers and optimized geometric parameters were seen to be in good agreement with the experimental data. Scale factors have been used in order to compare how the calculated and experimental data are in agreement. Theoretical infrared intensities were also reported.

Supporting information may be found in the online version of this article.

Keywords: Baicalein; Naringenin; flavonoids; infrared spectra; Raman spectra; HF; DFT

Introduction

Baicalein (5,6,7-trihydroxyflavone) (Fig. 1) is a plant flavonoid, formed *in vivo* by the metabolism of Baicalin by the cleavage of the glycoside moiety.[1] The action of Baicalein in the body includes inhibition of HIV-1 infection,[2] as well as antioxidant,[3] antifungal, antibacterial, and anti-inflammatory properties.[4] Baicalein is also known to inhibit lipoxygenases.[5] Baicalein has been isolated from *Scutellaria baicalensis*, and has been found to exhibit the enzyme a-glucosidase, thus preventing the absorption of dietary carbohydrates, consequently suppressing postprandial hyperglycemia.[6] Baicalein and Baicalin have both been found to interact with the GABAA receptor at the benzodiazepine-binding site, with an activity seven times less than that of 6-hydroxyflavone at the receptor complex.[7] Furthermore, the Baicalein molecule is interesting in itself due to the large range of intermolecular interactions present in the crystal lattice. The experimental charge density distribution of Baicalein has been determined from high-resolution X-ray diffraction data collected at 100 K.[8]

Naringenin (4,5,7-trihydroxyflavone) (Fig.1) is widely spread in nature and easily extracted from a number of different plants. Its protective effect against lipid peroxidation of membranes involved in several physiological and pathological disorders such as, aging, inflammation, atherosclerosis, ischemia, toxicity of oxygen and chemical substances has been largely studied.[9] Wang *et al*. showed that the rare earth complexes of Naringenin benzoyl hydrazone have certain antioxidative and cytotoxic activities.[10,11]

To the best of our knowledge, there is no detailed experimental and computational vibrational spectroscopic study on free Baicalein and Naringenin in the literature as yet. Therefore, the present study aims to give a complete description of the molecular geometry and molecular vibrations of Baicalein and Naringenin.

Computational details

Gaussian 98 quantum chemical software was used in all calculations.[12] The optimized structural parameters and vibrational wavenumbers for all the molecules were calculated by using HF and B3LYP functional with 6-31G(d,p) basis set. The vibrational modes were assigned on the basis of PED analysis using VEDA 4 program[13] and its visualization interface. Normal coordinate analysis of the title molecules has been carried out to obtain a more complete description of the molecular motions involved in the fundamentals. The calculated vibrational wavenumbers were scaled with the scale factors[14] (0,9614 for B3LYP) in order to figure out how the calculated data are in agreement with those of the experimental ones.

Experimental

The FT-IR and FT-Raman spectra of the molecules have been recorded between 4000-400 cm^{-1} region and 3500-5 cm^{-1} region, respectively. All FT-IR spectra were recorded at solid phase at room temperature (300 K) by using the KBr disc method. The Baicalein was purchased from Çayman Chemical Company Naringenin from MP Biomedicals with a stated purity of greater than 98%, and

* *Correspondence to: Ozan Unsalan, Istanbul University, Science Faculty, Department of Physics 34134, Vezneciler Istanbul, Turkey. E-mail: unsalan@istanbul.edu.tr*

a *Istanbul University, Science Faculty, Department of Physics 34134, Vezneciler Istanbul, Turkey*

b *Ahi Evran University, Art and Science Faculty, Department of Physics, 40040, Kirsehir, Turkey*

Journal of RAMAN SPECTROSCOPY

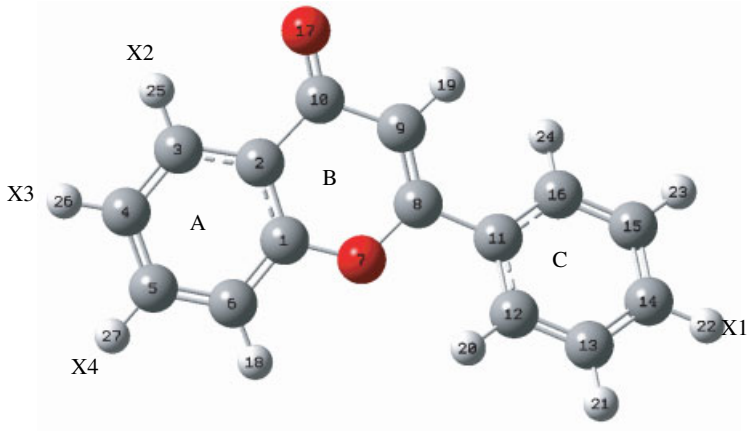

	X1	X2	X3	X4
Baicalein	H	OH	OH	OH
Naringenin	OH	OH	H	OH

Figure 1. Optimized molecular structure of Baicalein and Naringenin at B3LYP/6-31G(d,p). This figure is available in colour online at www.interscience.wiley.com/journal/jrs.

it was used without further purification. The infrared spectra of the samples were recorded on a Mattson 1000 FT-IR spectrometer which was calibrated using polystyrene bands. The FT-Raman spectra of the samples were recorded between 3500-5 cm^{-1} region on a Bruker FRA 106/S FT-Raman instrument using 1064 nm excitation from an Nd : YAG laser. The detector is a liquid nitrogen-cooled Ge detector.

Results and discussion

Molecular Geometries

The calculated optimized structures of all molecules are given in (Fig. 1) and their calculated geometric parameters are summarized in Table S1 (Supporting Information). X-ray crystallographic data for Baicalein are also given in Table S1. By taking into account that the molecular geometry in the vapour phase may be different from that in its solid phase, owing to extended hydrogen bonding and stacking interactions there is reasonable agreement between calculated and experimental geometric parameters. Crystal structure data of Baicalein were also used for Naringenin due to their skeletal analogy. Due to having neither reflection plane nor inversion center, calculations were utilized to the C_1 symmetries of the molecules. The most significant differences for the calculated geometries between the experimental ones are: 0.06 Å (HF), 0.044 Å (B3LYP) for the bond lengths, and 8.7° (HF), 6.1° (B3LYP) for the bond angles for Baicalein, and 0.06 Å (HF), 0.03 Å (B3LYP) for the bond lengths, and 3.9° (HF), 4.2° (B3LYP) for the bond angles for Naringenin.

In the flavonoid derivative, the four minima occurring at the torsional angles are identical because the phenyl group has no substituent at either the *ortho (o)* or *meta (m)* positions. For this reason, it was satisfactory to optimize only one of the four equivalent minima.[15]

$$(0+\alpha), (180-\alpha), (180+\alpha), (360-\alpha)$$

Rotational barrier with all the levels of theoretical approximation were performed along the O_7-C_8-C_{11}-C_{12} dihedral angle of corresponding molecules. The potential energy profile is presented in Fig. 2. Computational results showed that the maximum deviations of ring C from the A–B plane were (180°−28.3° = 151.7°) −28.3° (HF), (180°−19.9° = 160.1°) −19.9° (B3LYP) for Baicalein, and (180°−26.4° = 153.6°) −26.4° (HF), (0 + 17.4° = 17.4°) 17.4° (B3LYP) for Naringenin.

Vibrational wavenumbers

Both Naringenin and Baicalein molecules consist of 30 atoms, which have 84 normal modes. To the best of our knowledge, there are no detailed quantum chemical studies for the vibrational spectra of Naringenin and Baicalein. The resulting vibrational wavenumbers for the proposed vibrational assignments are given in Table 1. In Table 1, theoretical IR and Raman intensities were also given. All the calculated vibration values were scaled. Scale factors used here[14] were 0,9614 for B3LYP. Figures 3 and 4 indicate FT-Raman and infrared spectra of the titled molecules.

The theoretical Raman intensities (I_i^R) can be derived from the computed Raman scattering activities using the following equations:

$$I_i^R = C(\upsilon_0 - \upsilon_i)^4 . \upsilon_i^{-1} . B_i^{-1} . S_i \quad (1)$$

where: B_i is a temperature factor which accounts for the intensity contribution of excited vibrational states, and is represented by the Boltzmann distribution:

$$B_i = 1 - \exp\left(-\frac{h\upsilon_i c}{kT}\right) \quad (2)$$

In Eqn (1), υ_0 is the wavenumber of the laser excitation line (in this work, we have used the excitation wavenumber $\upsilon_0 = 9398.5\ cm^{-1}$, which corresponds to the wavelength of 1064 nm of a Nd : YAG laser), υ_i is the wavenumber of normal mode (cm^{-1}), while S_i is the Raman scattering activity of the normal mode Q_i. I_i^R i is given in arbitrary units (C is a constant equal to 10^{-12}). In Eqn (2) h, k, c, and T are Planck and Boltzmann constants, speed of light and temperature in Kelvin, respectively. The factor, B_i, was assumed to be 1, otherwise, the calculated Raman intensities for the bands below 300 cm^{-1} were extremely overestimated, in comparison to the experiment.[16]

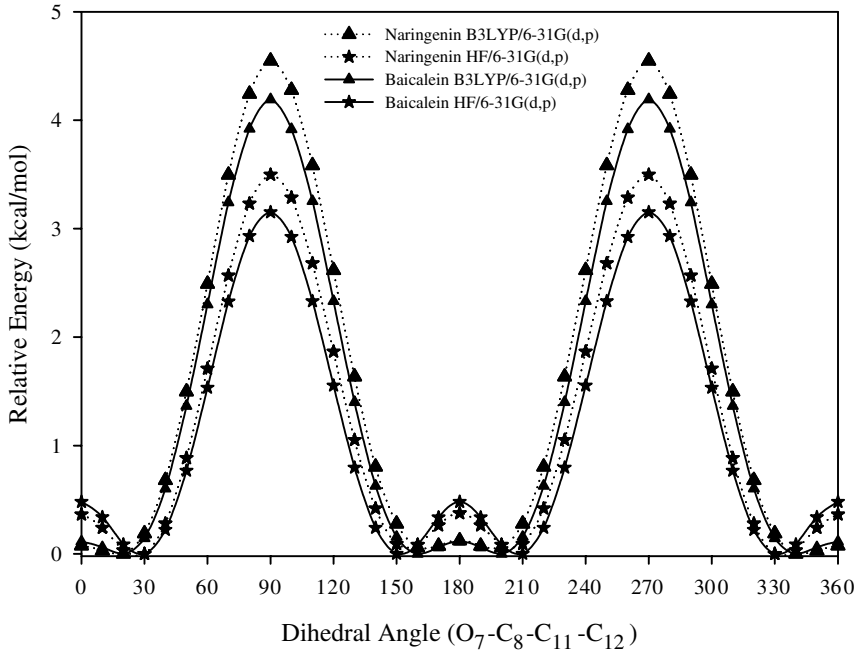

Figure 2. Potential energy profiles calculated at B3LYP and HF/6-31 G(d,p) level by internal rotation around the C_8-C_{11} bonds.

For Naringenin, one of four (ν(OH)) stretching modes were assigned at 3410 cm^{-1} in the IR spectrum as a broad band. Besides, this broad band may belong to all of ν(OH). None of the OH stretching modes were observed in the Raman spectrum. CH stretchings for ring C were observed at 3054 cm^{-1} (Ra-3038 cm^{-1}), 3081 cm^{-1} (Ra-3077 cm^{-1}), 3071 cm^{-1} (Ra-3075 cm^{-1}) and 3095 cm^{-1} (Ra-3100 cm^{-1} and 3090 cm^{-1} for B3LYP) in the IR spectrum. The only CH stretching modes for the ring A and ring B are observed at 3088 cm^{-1} (3085 cm^{-1}-B3LYP) and 3129 cm^{-1} (3118 cm^{-1}-B3LYP) in the IR spectrum, respectively. For ring C, the antisymmetric CH stretching modes are observed at 3081 cm^{-1} (3077 cm^{-1}-Ra, 3081 cm^{-1}-B3LYP) and 3071 cm^{-1} (3075 cm^{-1}-Ra, 3071 cm^{-1}-B3LYP) in the IR spectrum. The C=O stretching mode is observed at 1658 cm^{-1} with the strongest absorption in the IR spectrum, and 1660 cm^{-1} in the Raman spectra, and corresponds to 1679 cm^{-1} for the B3LYP calculations. The CC stretching modes for all rings were observed between 1019 cm^{-1} and 1618 cm^{-1} for IR and 1104 cm^{-1} and 1613 cm^{-1} for Raman, respectively. HCC bending modes for ring C were observed at 1452 cm^{-1} (1451 cm^{-1}-Ra, 1432 cm^{-1}-B3LYP), 1335 cm^{-1} (1329 cm^{-1}-B3LYP) and 1211 cm^{-1} (1235 cm^{-1}-Ra, 1220 cm^{-1}-B3LYP) in the IR spectrum. HOC bending modes for ring A were observed at 1161 cm^{-1} (1157 cm^{-1}-B3LYP), 1283 cm^{-1} (sh), (1284 cm^{-1} (weak) for Raman, 1283 cm^{-1}-B3LYP) and 1296 cm^{-1} (1297 cm^{-1}-B3LYP) for IR. Two HCC bendings for both A and B rings together were observed at 1183 cm^{-1} for IR and 1191 cm^{-1} for Raman (vw), (1177 cm^{-1}-B3LYP) respectively. CO stretching modes for ring B were observed at 1083 cm^{-1} (1074 cm^{-1}-B3LYP), 1388 cm^{-1} (1409 cm^{-1}-Ra, 1375 cm^{-1}-B3LYP) and 971 cm^{-1} (977 cm^{-1}-B3LYP) for IR and 1357 cm^{-1} (1363 cm^{-1}-B3LYP) for Raman. CO stretching modes for ring A were observed at 1034 (sh) cm^{-1} (1035 (w) cm^{-1} for Raman, 1049 cm^{-1}-B3LYP) and 824 cm^{-1} for IR (823 cm^{-1}-B3LYP). HCCC torsion modes for ring C were observed at 996 cm^{-1} (sh) (1000 cm^{-1} for Raman, 996 cm^{-1}-B3LYP), 964 cm^{-1} (964 cm^{-1}-B3LYP) and 745 cm^{-1} (744 cm^{-1}-B3LYP) for IR. The ring bending mode for ring C was observed at 918 cm^{-1} and 921 cm^{-1} (940 cm^{-1} for B3LYP) for IR and Raman, respectively. The CCO bending mode for ring B was observed at 896 cm^{-1} (890 cm^{-1} for B3LYP) both for IR and Raman as a perfect match. The OCCC out-of-plane bendings for ring A were observed at 596 cm^{-1} (596 cm^{-1}-B3LYP), 638 cm^{-1} (645 cm^{-1}-Ra, 633 cm^{-1}-B3LYP) for IR. The OCC bending for ring A was observed at 335 cm^{-1} for Raman only. Out-of-plane OH bending modes for ring A were observed at 463 cm^{-1} (470 cm^{-1}-B3LYP) and 449 cm^{-1} (sh) (445 cm^{-1}-B3LYP) for IR spectrum. The CCCC torsion of ring C was observed at 420 cm^{-1} and 425 cm^{-1} (397 cm^{-1}-B3LYP) for IR and Raman, respectively. HOCC torsions of A were observed at 273 cm^{-1} (250 cm^{-1}-B3LYP) and 204 cm^{-1} (185 cm^{-1}-B3LYP) for Raman only. The CCCC torsion mode of ring A was observed at 155 cm^{-1} (140 cm^{-1}-B3LYP) in the Raman spectrum only as a very weak band. The CCOC torsion between rings A and B was at 119 cm^{-1} (110 cm^{-1}-B3LYP) for Raman.

For Baicalein, none of the OH stretching modes were observed in the Raman spectrum. There are two CH stretching modes for ring A, one mode for B and four modes for ring C. Only the CH stretching mode for ring B was observed at 3117 cm^{-1} in the IR spectrum (Ra-3104 cm^{-1}, 3116 cm^{-1}-B3LYP). In the Raman spectrum one of the CH stretchings for ring C was observed at 3079 cm^{-1} (3105 cm^{-1}-B3LYP), where another was at 3058 cm^{-1} in (3057 cm^{-1} in the IR spectrum, 3050 cm^{-1}-B3LYP). One of the CH stretching modes for ring A was observed at 3075 cm^{-1} only in the Raman spectrum which corresponds to 3072 cm^{-1} for B3LYP. Characteristic IR absorbance peak for C=O stretching assigned as 1630 cm^{-1}. This peak was observed at 1619 cm^{-1} in the Raman spectra and corresponds to 1678 cm^{-1} for B3LYP. The CC stretching mode for ring C was at 1603 cm^{-1} (1608 cm^{-1}-B3LYP) and 1590 cm^{-1} (1608 cm^{-1}-B3LYP) in the IR and Raman spectra, respectively. CH bendings for ring C were at 1498 cm^{-1} (1500 cm^{-1}-Ra, 1501 cm^{-1}-B3LYP), 1158 cm^{-1} (1158 cm^{-1}-B3LYP) and 1084 cm^{-1} (1087 cm^{-1}-Ra, 1095 cm^{-1}-B3LYP) in the IR spectrum. The only CCO bending mode for ring B was observed at 1463 cm^{-1} and 1467 cm^{-1} for IR (1481 cm^{-1}-B3LYP) and Raman, respectively.

Table 1. Experimental and calculated wavenumbers of Baicalein and Naringenin (cm^{-1})

Baicalein								Naringenin							
		Experimental wavenumbers/cm^{-1}		Calculated wavenumbers/cm^{-1} B3LYP/6-31 G(d,p)						Experimental wavenumbers/cm^{-1}		Calculated wavenumbers/cm^{-1}			
Assignments	TED[c]/%	IR	Ra.	Unscld	Scld[a]	I_{IR}[d]	I_{Ra}[e]	Assignments	TED[c]/%	IR	Ra.	Unscld	Scld[b]	I_{IR}[d]	I_{Ra}[e]
OH stretching (A)	ν_{OH} (100)	–	–	3823	3675	12.41	9.39	OH stretching (A)	ν_{OH} (100)	–	–	3841	3693	19.24	6.22
OH stretching (C)	ν_{OH} (100)	–	–	3819	3672	17.51	0.45	OH stretching (A)	ν_{OH} (100)	–	–	3808	3661	29.45	0.28
OH stretching (A)	ν_{OH} (100)	–	–	3804	3657	11.08	0.52	OH stretching (A)	ν_{OH} (100)	3410	–	3755	3610	24.70	0.48
CH stretching (B)	ν_{CH} (97)	3117	3104	3241	3116	0.665	0.95	CH stretching (B)	ν_{CH} (98)	3129	–	3243	3118	0.475	0.28
CH stretching (C)	ν_{CH} (100)	–	3079	3230	3105	0.665	1.46	CH stretching (C)	ν_{CH} (87)	–	–	3226	3101	1.188	0.89
CH stretching (C)	ν_{CH} (89)	–	–	3212	3088	0.665	0.12	CH stretching (C)	ν_{CH} (88)	3095	3100	3214	3090	3.088	0.27
CH stretching (C)	ν_{CH} (98)	–	–	3211	3087	1.552	1.15	CH stretching (A)	ν_{CH} (99)	3088	–	3209	3085	0.475	0.08
CH stretching (A)	ν_{CH} (99)	–	–	3206	3082	0.887	0.57	CH stretching (C)	ν_{CH} (87)	3081	3077	3205	3081	6.176	0.30
CH stretching (A)	ν_{CH} (99)	–	3075	3195	3072	1.330	0.25	CH stretching (C)	ν_{CH} (96)	3071	3075	3194	3071	2.375	0.14
CH stretching (C)	ν_{CH} (96)	3057	3058	3172	3050	4.878	0.39	CH stretching (C)	ν_{CH} (96)	3054	3038	3184	3061	0.238	0.22
C=O stretching	$\nu_{C=O}$ (79)	1630	1619	1745	1678	100	0.40	C=O stretching	$\nu_{C=O}$ (84)	1658	1660	1746	1679	100	0.17
CC stretching (A-B)	ν_{CC} (40)			1688	1623	55.21	0.87	CC stretching (B)	ν_{CC} (48)	1618	1613	1691	1626	59.38	11.45
CC stretching (C)	ν_{CC} (52)	1603	1590	1673	1608	26.82	15.71	CC stretching (A)	ν_{CC} (46) +δ_{CCO} (12)	–	1604	1669	1605	19.71	1.27
CC stretching (A-B)	ν_{CC} (34)	–	–	1663	1599	92.68	13.81	CC stretching (C)	ν_{CC} (21)	–	–	1660	1596	0.000	2.20
CC stretching (A)	ν_{CC} (36) +δ_{CCC} (10)	–	–	1642	1579	19.512	8.64	CC stretching (A)	ν_{CC} (24)	1583	1586	1656	1592	2.850	13.17
CC stretching (C)	ν_{CC} (40)	–	–	1634	1571	1.330	8.04	CC stretching (C)	ν_{CC} (49)	1563sh	–	1631	1568	3.800	15.47
HCC bending (C)	δ_{HCC} (42) +ν_{CC} (11)	1498	1500	1561	1501	18.84	8.72	CC stretching (A)	ν_{CC} (20) +δ_{HCC} (17)	1504	1509	1545	1485	51.30	18.26
CCO bending (B)	δ_{CCO} (16) +δ_{HCC} (11) +ν_{CC} (11)	1463	1467	1540	1481	1.996	27.29	HCC bending (C)	δ_{HCC} (63)	–	1498	1538	1479	4.751	5.47
CC stretching (A)	ν_{CC} (16) +ν_{OC} (11) +δ_{HOC} (10)	–	1451	1505	1447	25.72	7.48	CCO bending (AB)	δ_{CCO} (28)	1472	–	1529	1470	4.276	9.94
CC stretching (C)	ν_{CC} (33) +δ_{HCC} (17)	1421	–	1477	1420	21.508	3.36	HCC bending (C)	δ_{HCC} (43)	1452	1451	1490	1432	6.888	2.77
OC stretching (A-B)	ν_{OC} (73)	1389	1401	1423	1368	10.86	3.52	CO stretching (B)	$\nu_{C=O}$ (16) +ν_{CO} (12)	1388	1409	1430	1375	17.10	1.13
CC stretching (A)	ν_{CC} (46) +δ_{HOC} (11)	–	1361	1404	1350	2.882	8.35	CO stretching (B)	ν_{CO} (22)	–	1357	1418	1363	7.838	2.01
CC stretching (C)	ν_{CC} (49) +δ_{HOC} (14)	1337	–	1386	1333	49.00	6.81	HCC bending (C)	δ_{HCC} (56)	1335	–	1382	1329	81.71	10.13
CO stretching (C)	ν_{CO} (15)	1313	1314	1375	1322	56.54	10.65	HOC bending (A)	δ_{HOC} (54) +$\nu_{C=O}$ (13)	–	–	1367	1314	0.950	1.79
HCC bending (C)	δ_{HCC} (27) +ν_{CC} (18)	–	1311	1332	1281	33.70	0.83	HOC bending (A)	δ_{HOC} (46) +ν_{CO} (13)	1296	–	1349	1297	44.89	22.44
CO stretching (C)	ν_{CO} (46)	–	1274	1321	1270	20.84	68.20	HOC bending (A)	δ_{HOC} (34) +ν_{CC} (13)	1283sh	1284	1335	1283	50.59	2.36
HCC bending (A)	δ_{HCC} (14) +δ_{HOC} (11)	1251	1251	1302	1252	31.92	4.22	HCC bending (B)	δ_{HCC} (41) +ν_{CC} (17)	–	–	1320	1269	76.48	0.51
HCC bending (B)	δ_{HCC} (43)	–	–	1277	1228	9.313	2.30	CC stretching (AB)	ν_{CC} (26) +δ_{HOC} (24)	1241	1247	1280	1231	6.651	23.45
CC sretching (A-B)	ν_{CC} (14) +ν_{CC} (12) +δ_{HOC} (13)	1219	1218	1267	1218	2.439	12.03	HCC bending (C)	δ_{HCC} (40)	1211	1235	1269	1220	3.088	4.18

Journal of RAMAN SPECTROSCOPY

Table 1. (*Continued*)

		Baicalein						Naringenin							
		Experimental wavenumbers/cm^{-1}		Calculated wavenumbers/cm^{-1} B3LYP/6-31 G(d,p)						Experimental wavenumbers/cm^{-1}		Calculated wavenumbers/cm^{-1}			
Assignments	TED[c]/%	IR	Ra.	Unscld	Scld[a]	I_{IR}[d]	I_{Ra}[e]	Assignments	TED[c]/%	IR	Ra.	Unscld	Scld[b]	I_{IR}[d]	I_{Ra}[e]
HOC bending (A)	δ_{HOC} (57)	1181	1183	1229	1182	35.25	4.88	HCC bending (AB)	δ_{HCC} (36) +ν_{CO} (21)	1183	1191	1224	1177	6.651	5.89
CO stretching (A-B)	ν_{CO} (34) +δ_{HCC} (26)	–	–	1206	1159	31.929	8.82	HCC bending (C)	δ_{HCC} (64)	–	–	1213	1166	8.076	7.06
HCC bending (C)	δ_{HCC} (42)	1158	–	1205	1158	8.426	4.43	HOC bending (A)	δ_{HOC} (14)	1161	–	1203	1157	21.61	7.35
HOC bending (C)	δ_{HOC} (45) +δ_{HCC} (20) +ν_{CC} (17)	–	–	1199	1153	67.40	5.74	CC stretching (A)	ν_{CC} (37) +δ_{HOC} (29)	–	–	1190	1144	0.238	0.68
HCC bending (A)	δ_{HCC} (40) +δ_{HOC} (27)	–	–	1191	1145	19.29	4.18	CC stretching (C)	ν_{CC} (31) +δ_{HCC} (17)	1102	1104	1175	1130	8.789	2.51
HCC bending (C)	δ_{HCC} (49) +ν_{CC} (31)	1084	1087	1139	1095	4.435	2.67	CO stretching (B)	ν_{CO} (16) +ν_{CC} (10)	1083	–	1117	1074	3.088	1.22
HCC bending (A-B)	δ_{HCC} (17) +δ_{CCO} (14)	–	–	1115	1072	20.62	2.58	CC stretching (C)	ν_{CC} (53) +δHCC (22)	–	–	1110	1067	4.988	1.26
CC stretching (A-B)	ν_{CC} (25) +ν_{OC} (19)	1065	1066	1113	1070	4.656	0.33	CO stretching (A)	ν_{CO} (19) +ν_{CC} (11)	1034sh	1035	1091	1049	35.62	2.89
HCC bending (A-B)	δ_{HCC} (13) +ν_{CC} (12) +ν_{OC} (10)	1014	1015	1055	1014	8.869	5.90	CC stretching (C)	ν_{CC} (12)	1019	–	1060	1019	1.663	4.77
CCC bending (C)	δ_{OCC} (66) +δ_{HCC} (11)	–	–	1030	990	1.330	3.90	HCCC torsion (C)	τ_{HCCC} (68) +τ_{CCCC} (17)	996sh	1000	1036	996	4.513	21.44
OC stretching (A-B)	ν_{OC} (17) +ν_{CC} (12)	970	969	997	959	5.543	10.29	CO stretching (B)	ν_{CO} (16)	971	–	1016	977	0.475	1.78
HCCC torsion (C)	τ_{HCCC} (89)	939	–	972	934	0.000	1.71	HCCC torsion (C)	τ_{HCCC} (78)	964	–	1003	964	0.000	2.40
HCCC torsion (C)	τ_{HCCC} (80) +τ_{CCCC} (13)	–	–	945	909	0.000	2.40	CCC bending (C)	δ_{CCC} (60) +ν_{CC} (23)	918	921	978	940	0.000	5.29
CCO bending (B)	δ_{CCO} (70)	890	890	922	886	1.552	0.59	HCCC torsion (C)	τ_{HCCC} (88)	–	–	939	903	0.475	0.83
HCCC torsion (B)	τ_{HCCC} (59) +γ_{OCCC} (16)	832	869	867	834	2.661	0.56	CCO bending (B)	δ_{CCO} (12)	896	896	926	890	7.126	1.00
HCCC torsion (C)	τ_{HCCC} (52) +γ_{OCCC} (13)	822	817	850	817	11.53	42.51	HCCC torsion (B)	τ_{HCCC} (54) +τ_{OCCC} (15)	853	–	894	859	26.36	4.62
CC stretching (C)	ν_{CC} (47) +ν_{OC} (22)	–	–	840	808	1.774	1.62	HCCC torsion (C)	τ_{HCCC} (71)	–	–	870	836	4.513	0.91
HCCC torsion (C)	τ_{HCCC} (74)	–	–	816	785	2.439	11.74	CO stretching (A)	ν_{CO} (16)	824	–	856	823	0.950	2.04
HCCC torsion (A)	τ_{HCCC} (69)	–	–	808	777	4.878	3.80	HCCC torsion (A)	τ_{HCCC} (74)	776	778	788	758	6.176	3.45
HCCC torsion (A)	τ_{HCCC} (65) +γ_{OCCC} (13)	761	757	785	755	8.647	0.66	HCCC torsion (C)	τ_{HCCC} (56) +τ_{CCCC} (16)	745	–	774	744	8.076	7.57
OCCC o.p.bending(A-B)	γ_{OCCC} (45) +τ_{HCCC} (18) +γ_{CCOC} (20)	731	–	764	735	1.552	2.65	O=CCC o.p. bending	$\gamma_{O=CCC}$(39)+τ_{HCCC}(27) +γ_{CCOC}(16)	729	732	748	719	0.475	0.14
CCCC torsion (B-C)	τ_{CCCC} (47) +γ_{OCCC} (13) +γ_{CCCC} (10)	713	713	732	704	0.443	1.71	HCCC torsion (C)	τ_{HCCC} (39) +τ_{CCCC} (22)	–	701	717	689	0.238	1.62
CCC bending (A-B)	δ_{CCC} (29) +δ_{CCO} (21)	–	682	725	697	1.109	4.99	CCO bending (A)	δ_{CCO} (12)	–	–	715	687	1.425	15.01
CCC bending (A-B)	δ_{CCC} (26) +ν_{CC} (10)	667	–	692	665	2.217	2.08	COC bending (B)	δ_{COC} (17) +δ_{CCC} (14)	680	–	705	678	6.176	11.03

(*continued overleaf*)

Table 1. (*Continued*)

Baicalein								Naringenin							
		Experimental wavenumbers/cm^{-1}		Calculated wavenumbers/cm^{-1} B3LYP/6-31 G(d,p)						Experimental wavenumbers/cm^{-1}		Calculated wavenumbers/cm^{-1}			
Assignments	TED[c]/%	IR	Ra.	Unscld	Scld[a]	I_{IR}[d]	I_{Ra}[e]	Assignments	TED[c]/%	IR	Ra.	Unscld	Scld[b]	I_{IR}[d]	I_{Ra}[e]
CCOC o.p.bending (A-B)	γ_{CCOC} (21) +γ_{OCCC} (11)	652	651	668	642	0.665	19.76	OCCC o.p. bending (A)	γ_{OCCC} (41) +τ_{OCCC} (19)	638	645	658	633	0.950	1.45
CCC bending (A-B-C)	δ_{CCC} (11) +τ_{CCCC} (10) +γ_{CCOC} (10)	632	634	659	634	0.000	3.59	CCOC o.p. bending (B)	γ_{CCOC}(27)+τ_{OCCC}(15) +τ_{CCCC}(10)	616	622	642	617	0.475	2.02
CCOC o.p. bending(B-C)	γ_{CCOC} (20)	–	–	649	624	0.000	100	CCOC o.p.bending(AB)	γ_{CCOC} (47) +τ_{OCCC} (27)	–	610	633	609	0.000	34.40
OCC bending (A-B)	δ_{OCC} (15) +δ_{CCO} (10)	615	–	637	612	0.222	7.49	CCO bending (B)	δ_{CCO} (22) +δ_{OCC} (11)	–	–	630	606	0.713	46.00
OCCC o.p.bending (A-B)	γ_{OCCC} (53)	–	–	632	608	1.552	13.00	CCC bending (C)	δ_{CCC} (56)	–	–	623	599	0.000	8.58
OCCC o.p.bending (A-B)	γ_{OCCC} (28) +γ_{CCOC} (25)	–	–	616	592	0.443	4.98	OCCC o.p. bending (A)	γ_{OCCC} (61) +τ_{HCCC} (15)	596	–	620	596	0.238	5.31
CCC bending (A-B-C)	δ_{CCC} (17)	564	–	582	560	2.439	2.87	CC stretching (A)	ν_{CC} (14) +ν_{CO} (10) +δ_{CCC} (10)	568	–	590	567	1.188	4.14
CCC bending (A-B-C)	δ_{CCC} (29)	554	556	552	531	1.552	4.10	OCC bending (AB)	δ_{OCC} (46) +δ_{CCC} (13)	557sh	526	570	548	9.739	18.54
OCC bending (A)	δ_{OCC} (18) +γ_{OCCC} (11)	501	502	520	500	1.330	27.79	CCC bending (A)	δ_{CCC} (20)	519	516	521	501	0.238	5.44
OCCC o.p. bending (C)	γ_{OCCC} (25) + $\delta_{CC=O}$ (11)	492	–	516	496	4.656	19.39	CCCC o.p. bending (B-C)	γ_{CCCC}(18)+δ_{CCC}(15) +δ_{COC}(10)+τ_{CCCC}(10)	483	–	498	479	17.57	14.87
CCC bending (A-B-C)	δ_{CCC} (22) +δ_{COC} (17)	459	460	489	470	4.213	10.05	OH o.p. bending (A)	γ_{OH} (79)	463	–	489	470	3.325	10.62
OCC bending (A-C)	δ_{OCC} (36) +τ_{HOCC} (16)	–	–	436	419	7.539	6.35	OH o.p. bending (A)	γ_{OH} (17)	449sh	–	463	445	0.475	3.94
HOCC torsion (A)	τ_{HOCC} (73)	–	416	433	416	22.83	2.26	CCCC torsion (C)	τ_{CCCC} (62) +τ_{HCCC} (45)	420	425	413	397	0.000	1.27
CCCC torsion (C)	τ_{CCCC} (65) +τ_{HCCC} (22)	–	402	419	403	0.222	3.37	OCCC o.p. bending (A)	γ_{OCCC} (18) +τ_{CCCO} (11)	–	–	405	389	0.000	3.23
CCC bending (C)	δ_{CCC} (25)+δ_{CCC}(15) +δ_{COC}(11)+ν_{CC}(10)	–	381	394	379	1.774	9.77	OCCC o.p. bending (A)	γ_{OCCC} (28) +τ_{CCCO} (12)	–	360	384	369	0.475	10.03
HOCC torsion (C)	τ_{HOCC} (94)	–	–	377	362	30.82	11.54	OCC bending (A)	δ_{OCC} (51) +δ_{CCC} (17)	–	335	337	324	2.138	3.87
HOCC torsion (A)	τ_{HOCC} (93)	–	–	374	360	15.96	14.81	OCC bending (B)	δ_{OCC} (16) +δ_{CCC} (12)	–	–	327	314	1.663	13.24
OCC bending (A)	δ_{OCC} (28)	–	–	350	336	1.774	87.79	OCC bending (A)	δ_{OCC} (78)	–	–	305	293	3.325	100
OCC bending (A)	δ_{OCC} (18) +γ_{CCCC} (10)	–	–	338	325	1.330	91.36	CCCC torsion (AB)	τ_{CCCC}(36)+τ_{CCOC} (20) +τ_{CCCO} (12)	–	–	304	292	1.663	39.88
CC=O bending (A-B)	$\delta_{CC=O}$ (14)	–	298	318	306	0.443	54.80	HOCC torsion (A)	τ_{HOCC} (64)	–	–	294	283	1.188	44.53
CCCC torsion (A-B)	τ_{CCCC} (24) +τ_{CCOC} (18)	–	275	290	279	0.443	40.64	HOCC torsion (A)	τ_{HOCC} (25) +δ_{CCC} (12)	–	273	260	250	9.026	26.14
CCCO torsion (A-B)	τ_{CCCO} (28) +δ_{CCO} (15)	–	250	247	237	0.222	0.97	CC stretching (B-C)	ν_{CC} (18) +δ_{CCC} (10)	–	250	247	237	5.938	1.75
CCO bending (A-B)	δ_{CCO} (24) +δ_{CCC} (13) +τ_{CCCO} (11)	–	227	235	226	0.222	2.84	CCO bending (AB)	δ_{CCO} (25)	–	–	235	226	9.026	1.98
CC stretching (AB-C)	ν_{CC} (24)	–	221	232	223	0.000	3.23	CCCC torsion (BC)	τ_{CCCC}(12)+τ_{CCCC}(11)+ τ_{HOCC}(10) +τ_{CCCO} (10)	–	215	220	212	30.64	0.87

Journal of RAMAN SPECTROSCOPY

Table 1. (*Continued*)

Baicalein								Naringenin							
		Experimental wavenumbers/cm^{-1}		Calculated wavenumbers/cm^{-1} B3LYP/6-31 G(d,p)						Experimental wavenumbers/cm^{-1}		Calculated wavenumbers/cm^{-1}			
Assignments	TED[c]/%	IR	Ra.	Unscld	Scld[a]	I_{IR}[d]	I_{Ra}[e]	Assignments	TED[c]/%	IR	Ra.	Unscld	Scld[b]	I_{IR}[d]	I_{Ra}[e]
CCCC torsion	τ_{CCCC} (56) + γ_{OCCC} (14)	–	200	214	206	0.443	1.36	HOCC torsion (A)	τ_{HOCC} (59) + τ_{CCCC} (43)	–	204	192	185	2.613	0.56
CCCC torsion (B)	τ_{CCCC} (60)	–	123	159	153	0.443	2.94	CCCC torsion (A)	τ_{CCCC} (43) + τ_{HOCC} (23)	–	155	146	140	2.850	1.21
CCOC torsion (A)	τ_{CCOC} (39)	–	99	108	104	0.222	1.71	CCOC torsion (AB)	τ_{CCOC}(31)+τ_{CCCC} (14) + τ_{CCCC} (11)	–	119	114	110	0.238	0.96
OCC bending (AB-C)	δ_{OCC} (21) + τ_{CCCC} (18) + δ_{CCC} (15)	–	–	84	81	0.443	1.59	CCCC torsion (B-C)	τ_{CCCC}(21)+δ_{OCC}(16) + τ_{CCOC}(14)+δ_{CCC}(10)	–	–	91	87	0.238	0.96
OCCC torsion (A-B)	τ_{OCCC} (29)	–	–	73	70	0.222	1.15	OCC bending (B-C)	δ_{OCC} (22) + τ_{CCCC} (12) + γ_{CCCC} (11)	–	–	83	80	0.000	1.22
COCC torsion (A-B)	τ_{COCC} (43) + γ_{CCCC} (17) + τ_{CCCO} (12)	–	–	41	39	0.000	1.19	COCC torsion (B-C)	τ_{COCC}(33)+τ_{OCCC}(24) + τ_{CCOC}(10)	–	–	43	41	0.000	1.44
OCCC torsion (AB-C)	τ_{OCCC} (89)	–	–	29	28	0.443	1.24	OCCC torsion (B-C)		–	–	29	28	0.238	0.76

[a,b] Taken from Ref. [14], 0,9614 scale factor used for B3LYP,
[c] Total energy distribution calculated B3LYP/6-31G(d,p) level (VEDA4 software for TED analysis),
[d] Relative absorption intensities normalized with highest peak absorption equal to 100,
[e] Relative Raman intensities calculated by Eqn (1) and normalized to 100, ν: stretching; δ: in-plane bending; γ: out-of-plane bending; τ: torsion; I_{IR}: IR intensities, I_{RA}: Raman intensities.

Journal of RAMAN SPECTROSCOPY

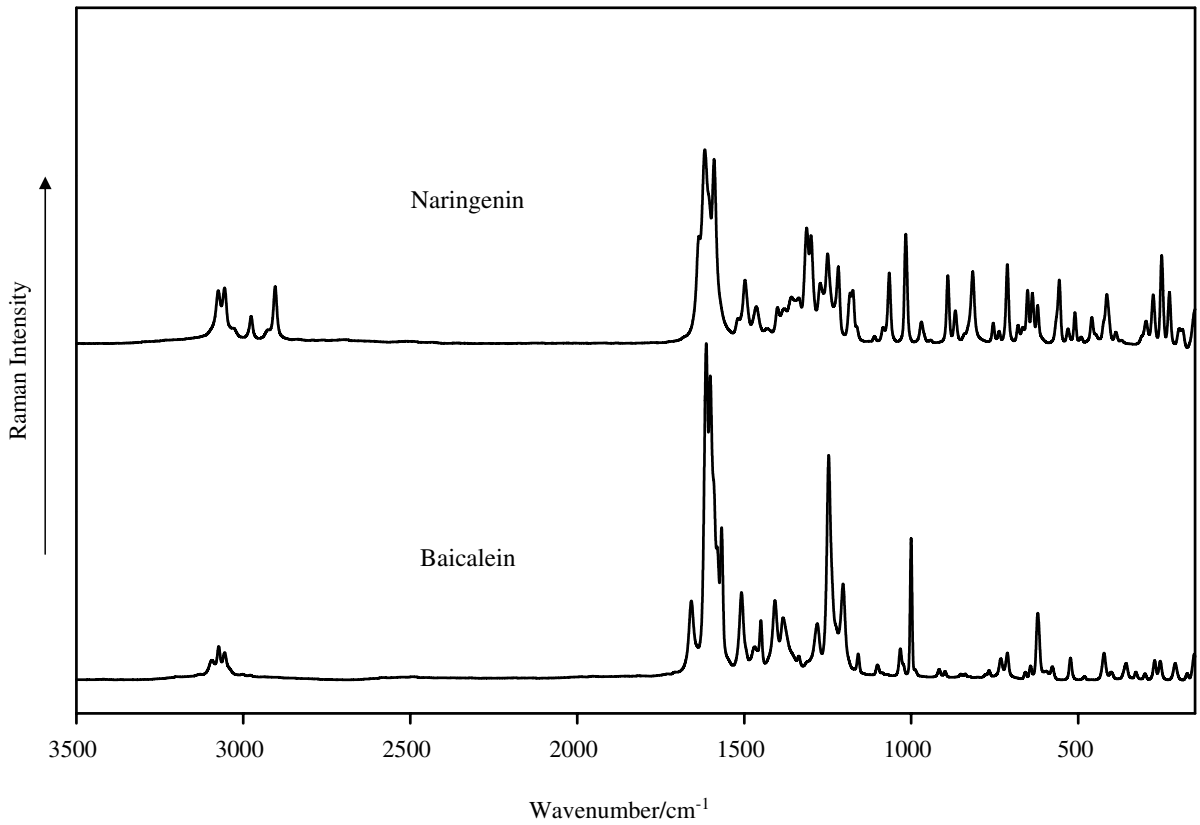

Figure 3. FT-Raman spectra of Baicalein and Naringenin.

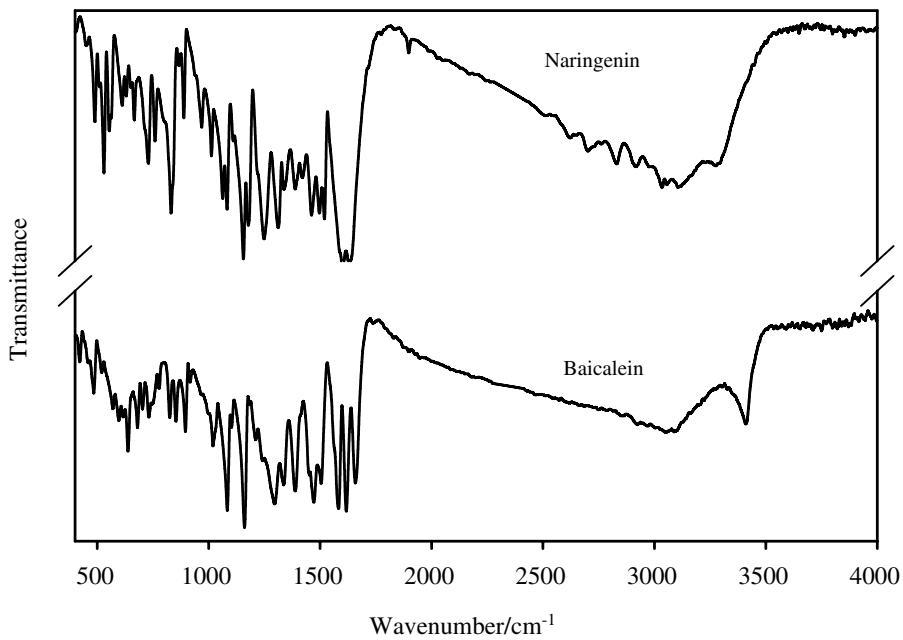

Figure 4. Infrared spectra of Baicalein and Naringenin.

The CO stretching modes for ring C were assigned at 1313 cm^{-1} in the IR spectrum (1314 cm^{-1}-Ra, 1322 cm^{-1}-B3LYP) and 1274 cm^{-1} (1270 cm^{-1}-B3LYP) for the Raman spectrum. The in-plane HOC bending mode for ring A was at 1181 cm^{-1} and 1183 cm^{-1} for IR and Raman, respectively, which matched well with the scaled B3LYP results (1182 cm^{-1}). CO stretchings for A and B rings together were calculated at 1159 cm^{-1} for B3LYP and none of them was observed in the experimental spectra. The HCCC torsion mode for ring C was observed at 939 cm^{-1} (934 cm^{-1}-B3LYP), the HCCC torsion mode for ring B was at 832 cm^{-1} (869 cm^{-1}-Raman, 834 cm^{-1}-B3LYP) and the HCCC torsion mode for ring A was at 761 cm^{-1} (757 cm^{-1}-Raman, 755 cm^{-1}-B3LYP) in the IR spectrum. The OCCC out-of-plane bending mode for both rings A and B assigned as 731 cm^{-1} in the IR spectrum (735 cm^{-1}-B3LYP). The CCCC torsion mode for both rings B and C was observed at 713 cm^{-1} for both IR and Raman spectra (704 cm^{-1}-B3LYP). The in-plane OCC bending mode for A and B rings was at 615 cm^{-1} for IR (612 cm^{-1}-B3LYP). The out-of-plane OCCC bending modes for A and B rings were calculated at 608 cm^{-1} and 592 cm^{-1} for scaled B3LYP. The OCC in-plane bending mode for ring A was assigned as 501 cm^{-1} (502 cm^{-1}-Raman ad 500 cm^{-1} for B3LYP) in the IR spectrum. The HOCC torsion mode for ring A was observed at 416 cm^{-1} in the Raman spectrum (416 cm^{-1}-B3LYP). The CCC bending mode for ring C was observed at 381 cm^{-1} in the Raman spectrum (379 cm^{-1}-B3LYP). CC=O bending (AB) was at 298 cm^{-1} (306 cm^{-1}-B3LYP), CCCC torsion (AB) at 275 cm^{-1} (279 cm^{-1}-B3LYP), CCCO torsion (AB) at 250 cm^{-1} (237 cm^{-1}-B3LYP), CCO bending (AB) at 227 cm^{-1} (226 cm^{-1}-B3LYP), CC stretching (the bond that connects rings B and C) at 221 cm^{-1} (223 cm^{-1}-B3LYP), CCCC torsion (B) at 123 cm^{-1} (153 cm^{-1}-B3LYP) and CCOC torsion (A) at 99 cm^{-1} (104 cm^{-1}-B3LYP) in the Raman spectrum.

Summary and conclusion

The optimized structural parameters, vibrational wavenumbers and corresponding vibrational assignments of Baicalein and Naringenin were examined by *ab initio* HF and DFT methods with B3LYP functional at 6-31G(d,p) basis set level for the first time. TED (Total Energy Distribution) analysis was done by using VEDA 4 software in order to assign the vibrational modes correctly. FT-IR and FT-Raman spectra of the compounds were recorded and theoretical IR intensities were also reported. The results showed that experimental and theoretical data were in good agreement.

Supporting information

Supporting information may be found in the online version of this article.

References

[1] S. Chen, Q. Ruan, E. Bedner, A. Deptala, X. Wang, T. C. Hsieh, F. Traganos, Z. Darzynkiewicz, *Cell Proliferation* **2001**, *34*, 293.
[2] B. Q. Li, T. Fu, Y. Dongyan, J. A. Mikovits, F. W. Ruscetti, J. M. Wang, *Biochem. Biophys. Res. Commun.* **2000**, *276*, 534.
[3] Z.-H. Shao, T. L. Vanden Hoek, Y. Qin, L. B. Becker, P. T. Schumacker, C. Q. Li, L. Dey, E. Barth, H. Halpern, G. M. Rosen, C.-S. Yuan, *Am. J. Physiol. Heart Circ. Physiol.* **2002**, *282*, H999.
[4] T. Hong, G.-B. Jin, S. Cho, J.-C. Cyong, *Planta Med.* **2002**, *68*, 268.
[5] I. Startchik, D. Morabito, U. Lang, M. F. Rossier, *J. Biol. Chem.* **2002**, *277*, 24265.
[6] T. Nishioka, J. Kawabata, Y. Aoyama, *J. Nat. Prod.* **1998**, *61*, 1413.
[7] J. Ai, K. Dekermendjian, X. Wang, M. Nielsen, M.-R. Witt, *Drug Dev. Res.* **1997**, *41*, 9.
[8] D. E. Hibbs, J. Overgaard, C. Gatti, T. W. Hambley, *New J. Chem.* **2003**, *27*, 1392.
[9] S. Tommasini, D. Raneri, R. Ficarra, M. L. Calabrò, R. Stancanelli, P. Ficarra, *J. Pharm. Biomed. Anal.* **2004**, *35*, 379.
[10] B. D. Wang, Z. Y. Yang, Q. Wang, T. K. Cai, P. Crewdson, *Bioorg. Med. Chem.* **2006**, *14*, 1880.
[11] B. D. Wang, Z. Y. Yang, Y. Wang, *Synth. React. Inorg. Met.-Org. Chem.* **2005**, *35*, 533.
[12] M. J. Frisch, G. W. Trucks, H. B. Schlegel, G. E. Scuseria, M. A. Robb, J. R. Cheeseman, V. G. Zakrzewski, J. A. Montgomery Jr, R. E. Stratmann, J. C. Burant, S. Dapprich, J. M. Millam, A. D. Daniels, K. N. Kudin, M. C. Strain, O. Farkas, J. Tomasi, V. Barone, M. Cossi, R. Cammi, B. Mennucci, C. Pomelli, C. Adamo, S. Clifford, J. Ochterski, G. A. Petersson, P. Y. Ayala, Q. Cui, K. Morokuma, D. K. Malick, A. D. Rabuck, K. Raghavachari, J. B. Foresman, J. Cioslowski, J. V. Ortiz, A. G. Baboul, B. B. Stefanov, G. Liu, A. Liashenko, P. Piskorz, I. Komaromi, R. Gomperts, R. L. Martin, D. J. Fox, T. Keith, M. A. Al-Laham, C. Y. Peng, A. Nanayakkara, C. Gonzalez, M. Challacombe, P. M. W. Gill, B. G. Johnson, W. Chen, M. W. Wong, J. L. Andres, M. Head-Gordon, E. S. Replogle, J. A. Pople, *Gaussian 98, Revision A.9*, Gaussian: Pittsburgh, **1998**.
[13] M. H. Jamróz, Vibrational energy distribution analysis VEDA 4, Warsaw, **2004**.
[14] A. P. Scott, L. Raom, *J. Phys. Chem.* **1996**, *100*, 16502.
[15] A. Mantas, E. Deretey, F. H. Ferretti, M. Estrada, I. G. Csizmadia, *J. Mol. Struct. (Theochem)* **2000**, *504*, 77.
[16] R. Wysokinski, K. Hernik, R. Szostak, D. Michalska, *Chem. Phys.* **2007**, *333*, 37.